Produced by the Water and Environmental Engineering group, University of Southampton, in collaboration with HR Wallingford

BOOKLET

Assessing the effects of debris accumulations at river bridges

September 2018

Prepared and edited by

Francisco Nicolas Cantero-Chinchilla, Gustavo A. M. de Almeida and Manuela Escarameia as part of the NERC-ERIIP grant DEBRIEF (NE/R009015/1)



Acknowledgements

This guide is an output of the project "Debris Effects on Bridge Piers and Flooding" (DEBRIEF), which was funded by NERC under the ERIIP programme (NE/R009015/1).

Lead authors and editors: Gustavo de Almeida & Francisco N. Cantero-Chinchilla (University of Southampton); Manuela Escarameia (HRWallingford).

We acknowledge the valuable contribution of the following staff from Network Rail who contributed to the project.

Steve Roffe, Senior Engineer

Kevin Giles, Senior Asset Engineer

Richard Newell, Senior Asset Engineer

Produced by the Water and Environmental Engineering group, University of Southampton, in collaboration with HR Wallingford

Disclaimer

This guide has been prepared by the University of Southampton, in collaboration with HRWallingford and Network Rail (hereafter referred to as 'the authors').

It has been produced for the benefit of stakeholders involved in the design and assessment of risks of bridges subject to the accumulation of large wood debris.

The information contained is believed to be correct at the time of publication, but may need to be updated as new research becomes available in the future.

The authors make no warranties, express or implied, that compliance with the contents of this document is sufficient on its own to ensure safe systems work or operation.

The authors will not be held responsible for any loss or damage arising from the adoption or use of anything referred to or contained in this publication.

Published by the University of Southampton

University Rd, Southampton, SO171BJ, UK

September 2018

Contents

1. INTRODUCTION 5

1.1. *How to use this guide?* 6

1.2. *Definitions used in this guide* 8

2. ESTIMATING THE POTENTIAL SIZE OF DEBRIS JAMS AT BRIDGE PIERS 9

2.1. *Determining the dimensions of debris accumulations at single-piers* 9

2.2. *Estimating the size of the design log* 12

3. ASSESSING THE EFFECTS OF DEBRIS JAMS ON PIER LOADINGS 14

4. ASSESSING THE INFLUENCE OF DEBRIS ON LOCAL SCOUR AT BRIDGE PIERS 18

4.1. *Estimation of local scour in absence of debris jams* 19

4.2. *Estimation of scour induced by debris jams* 20

5. THE EFFECTS OF DEBRIS ON AFFLUX 22

5.1. *Understanding afflux* 22

5.2. *Theoretical background* 23

6. REFERENCES 25

APPENDIX A: CASE STUDY ILLUSTRATING THE ASSESSMENT OF THE BRIDGE PIER SCOUR 28

A1. Llangadog viaduct. River Sawdde, Llangadog, Wales, UK. 28

APPENDIX B: MATHEMATICAL RELATIONS USED TO COMPUTE AFFLUX (*DEBRIS-Afflux Calculator v*1.0) 31

Trapezoidal cross-sectional open channels 31

APPENDIX C: *DEBRIS-Afflux Calculator v*1.0 33

APPENDIX D: GLOSSARY OF TERMS AND ABBREVIATIONS 42

1. INTRODUCTION

This guide is concerned with the problem of the accumulation of floating wood debris at the front of bridge piers located in rivers (hereafter indistinctly referred to as wood debris or debris for simplicity). These debris accumulations are a potential hazard for the stability of bridges and are often responsible for increasing the risk of flooding. Wood debris accumulations modify the flow characteristics in the vicinity of piers, increasing the depth of scour and lateral loadings on piers, the combination of which can severely compromise the stability of the bridge infrastructure. In addition, debris jams at piers lead to an increase in upstream water levels (as illustrated **Figure 1** and hereafter referred to as *afflux*), an effect that can extend far from the bridge through backwater and produce substantial change in the risk of flooding of adjacent areas. This phenomenon is particularly relevant in urban areas, where the value of assets, people exposure and the number of bridges are typically highest.

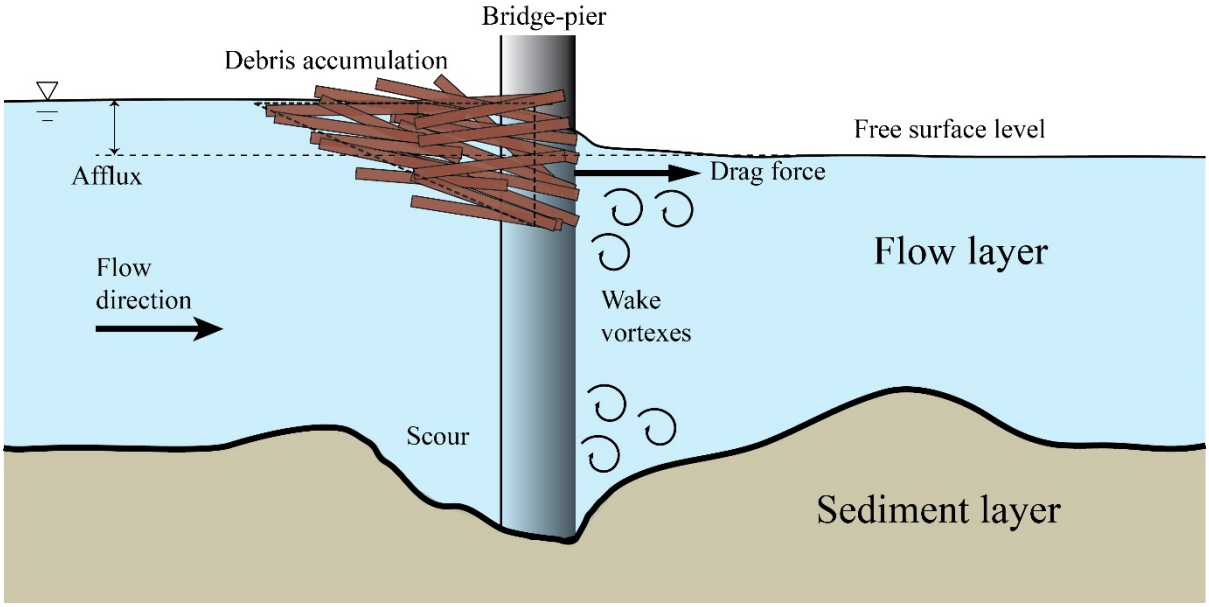


Figure 1. Sketch of a debris jam at the front of a bridge pier and its consequences.

Some studies have indicated that the formation of debris jams is one of the main causes for bridge failures, contributing to approximately one-third of bridge collapses in the UK, Ireland and the US (Diehl, 1997; Benn, 2013). The evaluation of the potential for large accumulations to develop, as well as the assessment of the above-mentioned effects, is therefore desirable to help mitigate the risk of infrastructure failure, as well as for the design of future river bridge infrastructures that are more resilient to extreme weather events (**Figure 2**).



Figure 2. Example of floating debris accumulation at the front of the bridge pier at the Lower Ashenbottom viaduct [adapted from Benn (2013)]

1.1. *How to use this guide?*

This guide aims to provide design and practising engineers with new tools to evaluate the potential implications of the formation of wood debris accumulations at bridge piers. The scope of the guide is limited to the advances recently achieved in the definition of the geometry of debris accumulations and related methods that can be derived from this information. While other published methods are mentioned and used as part of this document, the guide is not aimed at providing a comprehensive description of other published techniques for the estimation of scour, hydrodynamic loadings and afflux. Therefore, the guide should be used to complement other methodologies that are already available in the literature. For example, while we provide new evidence to support the estimation of the increase in scour depth that results from the accumulation of debris at piers, other methodologies need to be used in order to assess scour depths with no debris in place.

The recommendations provided in this guide refer exclusively to the problem of wood debris (e.g. trunks and branches of fallen trees) that collect around bridge piers after being transported in rivers floating near the water surface. While it is recognised that a number of debris jams are formed by the collection other types of debris (e.g. household items, vehicles, containers or

trash in general), problems that occur as a result of these types of debris are not covered here. It is however important to highlight that many debris accumulations are formed by a combination of both types of debris, usually with woody debris providing a frame that entraps other floating objects. Similarly, the focus of the guide is exclusively on debris accumulations at single-piers. Whilst some of the recommendations provided in this guide can be used to inform decisions involving other scenarios (e.g. span accumulations), such extrapolations should be done with caution.

The organization of this guide is as follows:

- Section 1 provides a brief introduction to the problems associated with the accumulation of large wood debris at bridge piers. The definitions of the main terms used in this guide can be also consulted from the end of this section.
- Section 2 describes methods that can be used to estimate the potential size (width, depth and length) of debris accumulations formed at single piers.
- Section 3 uses the methods presented in the previous section, as well as other information regarding the coefficient of drag of debris accumulations, to draw a simple method to assess hydrodynamic loadings exerted on bridges by the combined blockage imposed by the debris jam and pier.
- Section 4 provides information to aid the assessment of the effects of wood debris accumulations on scour depth around bridge piers.
- Section 5 contains context and theoretical information about the afflux phenomenon, presenting both general and specific formulations. A short user-manual to a software developed as part of the DEBRIEF project (NE/R009015/1) to assess afflux from debris is also included at the end of this section.
- Section 6 provides the list of references cited throughout this booklet.
- Appendix A contains an illustrative case study to help the reader understand and use the guide.
- Appendix B describes the mathematical relations used to compute afflux in the software developed as part of this guide.
- Appendix C presents a user guide and background for using the standalone software developed by the University of Southampton ('DEBRIS-Afflux Calculator v1.0'). The software allows users to estimate afflux for single, centred piers affected by debris accumulations in different cross-sectional river shapes.

- Appendix D defines the key terms and acronyms employed in this guide.

1.2. *Definitions used in this guide*

The main specific terminology employed in this guide is described below:

- *Maximum scour*: maximum depth of scour at the front of the pier under equilibrium conditions. It is denoted by d_{se}, and has units of length.
- *Actual scour:* scour depth at the front of the pier at a certain instant in time before equilibrium is reached. It is denoted by d_s, and has units of length.
- *Afflux:* the increase in the upstream water level of a river channel caused by the presence of the pier and debris jam. It is denoted by Δh, and represents the difference in flow depth h relative to the hypothetical condition where the pier and debris are not present.
- *Drag force*: force that the flow exerts on the debris accumulation and/or pier. It is denoted by F_D, and has units of force.

Appendix C presents a more detailed glossary for other terms, variables, and definitions used in this guide.

2. ESTIMATING THE POTENTIAL SIZE OF DEBRIS JAMS AT BRIDGE PIERS

The effects of debris jams described in this guide (i.e. increased loadings, scour and afflux) are known to depend critically on the size of debris accumulations formed at the pier. In order to be able to assess the implications of debris accumulations on each of these effects, it is therefore crucial to perform an evidence-based analysis of the potential dimensions that a debris jam can reach at given piers. To this end, two sources of well-documented evidence are currently available. The first refers to over 2,500 observations of debris accumulations in North American rivers as reported by the Federal Highway Administration (Diehl, 1997) and National Cooperative Highway Research Program (Lagasse et al., 2010). The second source of evidence comes from an extensive set of laboratory experiments conducted at the University of Southampton (Panici and de Almeida, 2018), in which the processes of formation and growth of debris accumulations have been analysed under a wide range of flow conditions and with debris of different characteristics. While field observation provides real-world data that is free from scale effects and includes the complexity of natural environments, most of observations available are limited to the moment of the site visit and may therefore miss the maximum dimensions reached by debris jams during flood events. On the other hand, experiments provide the opportunity to observe the entire process of growth of jams under controlled laboratory conditions, as well as to explore the influence that particular factors may have on the final size of accumulations. However, laboratory tests only represent an idealised approximation to real-world problems. Despite these differences, remarkable agreement has been found from the comparison between field and a group of experiments adopting a more realistic representation of debris (Panici and de Almeida, 2018).

Debris accumulations at bridges can be classified as: (*i*) single-pier (when debris jam is held by a single pier), (*ii*) span-blockage (in which case two or more piers, abutments or banks support the accumulation) and (iii) deck-blockage. This guide focuses on single-pier accumulations, which has been cited as the most common type of debris accumulations (Diehl, 1997; Lyn et al., 2007).

2.1. *Determining the dimensions of debris accumulations at single-piers*

Field observations and laboratory results concur that the majority of debris jams that are formed at single-piers by the successive collection of woody debris transported in rivers have

a shape that can be described as an inverted half-cone, as schematically shown in **Figure 3**. Such a geometry can be defined by the three dimensions *W* (width), *H* (height) and *K* (length), which are also illustrated in **Figure 3**.

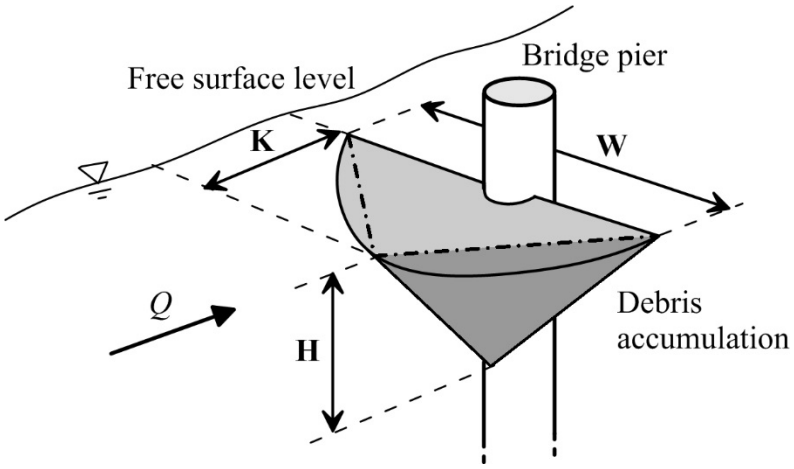


Figure 3. Idealised inverted half-conical model of a single-pier debris accumulation at bridge pier.

The potential dimensions of large wood debris accumulations depend strongly on the length of wood debris entrained and transported by the river. Field observations (Diehl, 1997; Lagasse et al, 2010) indicate that many accumulations contain long logs that rest on the pier perpendicular to the flow (hereafter referred to as 'key structural logs' or simply 'key logs'), which then collect and hold other smaller logs and branches. The same observations have been used by Diehl (1997) and Lagasse et al (2010) to recommend that the width of single-pier debris accumulations can be determined by the length of the longest log, that is $W/L=1$ (where L is the length of the longest piece of debris transported by the river at the location of the bridge). While this rule provides a ballpark figure to the width of accumulations, Diehl (1997) also reports a limited set of cases in which accumulations wider than the length of the longest log were observed. With regards to the depth *H* of accumulations, American guidelines report that they can, "*under some circumstances*" (Diehl, 1997) and "*often*" (Lagasse et al., 2010), extend from the water surface to the riverbed.

Panici and de Almeida (2017) conducted 570 laboratory experiments in which debris pieces were continuously introduced into a rectangular flume at the centre of which a model pier of circular shape was installed. In these experiments, debris of both uniform and non-uniform length were used. Experiments with debris having non-uniformly distributed length were designed to mimic the distribution of lengths of logs that is commonly observed in many rivers.

In all experiments the accumulations grew by the successive collection of debris pieces until a maximum size was reached and the whole accumulation was removed from the pier by the flow. This maximum dimension was recorded and correlated to the characteristics of flow and debris. The results of these experiments are presented in **Figure 4**, which shows the three dimensions of the accumulations (made dimensionless with L: W/L, H/L, K/L) as a function of $Fr_L = U/\sqrt{gL}$ (where U is the reference streamwise velocity of the flow and g the acceleration due to gravity).

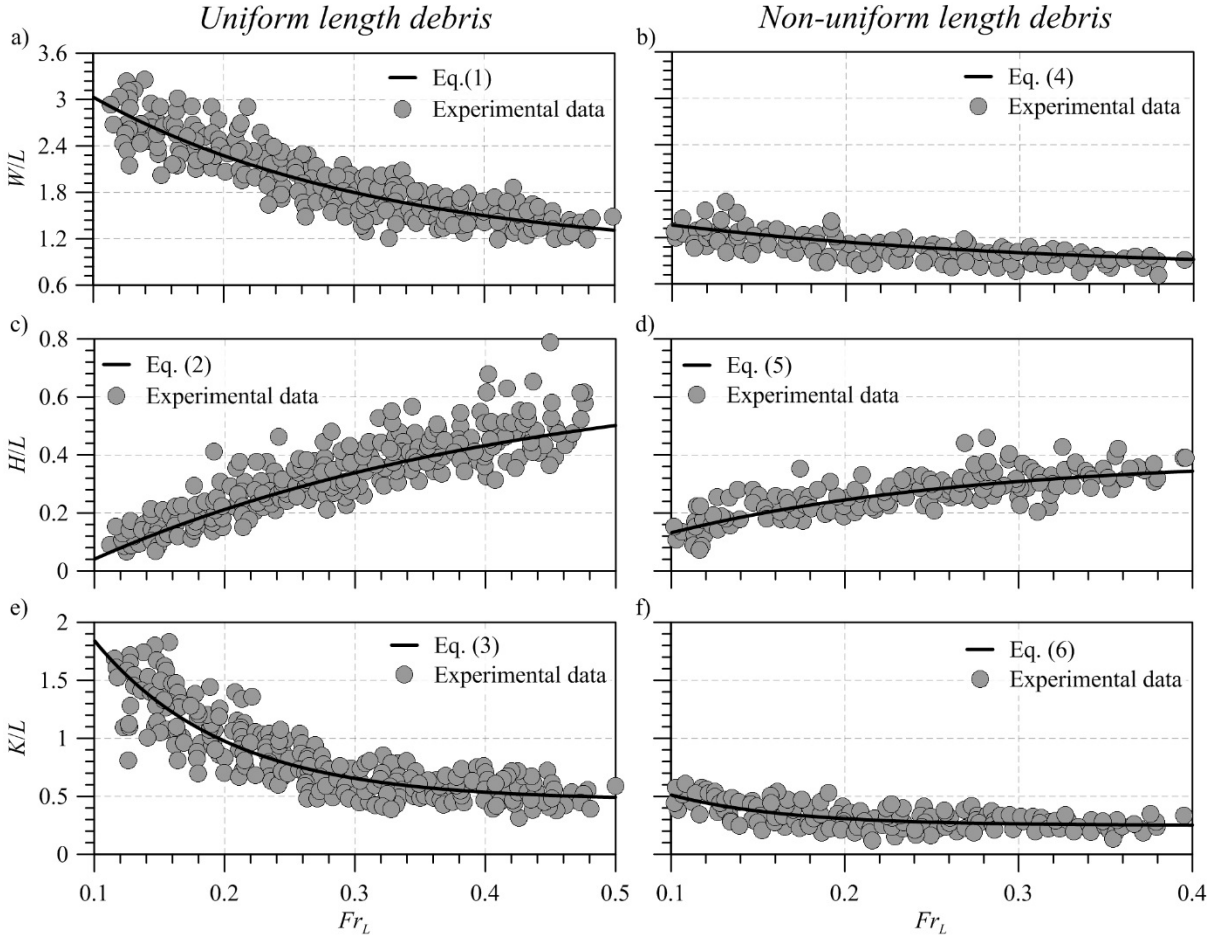


Figure 4. Results of laboratory experiments by Panici and de Almeida (2018). On the left, results obtained from the experiments with debris of uniform length: W/L (a), H/L (c) and K/L (e). On the right, results of experiments with debris of varied lengths: W/L (b), H/L (d) and K/L (f) (in which case L represents the length of the longest debris piece or 'key log').

The results obtained with debris pieces of non-uniform length display values of the dimensionless widths close to the W/L=1 previously reported by field observations, although they show that this value varies approximately within the 0.8~1.3 range depending on Fr_L. While this agreement confirms the reliability of laboratory tests, the results of the experiment

provide a more detailed analysis of how the dimensions of debris accumulations depend on particular characteristics of flow and debris pieces. For example, results from tests with debris of uniform length show substantially wider accumulations compared to non-uniform tests (i.e. approximately ranging from 1.3 to 3.0 times the length of the debris pieces). Whilst the transport of debris of uniform length is unlikely to occur in natural rivers, such situation may arise if wood material from logging activities is entrained and transported during flood events. The results of accumulations produced by uniform length debris can also be used as a guide to the maximum potential size (i.e. worst-case scenario) of accumulations that can be produced by the mechanisms of self-assembly reproduced by these experiments. The regression curves shown in **Figure 4**, which can be used for the estimation of the size of debris jams, are described by the following expressions

$$\frac{W}{L} = 0.99 + 3.24\,\mathrm{e}^{-4.625 Fr_L} \tag{1}$$

$$\frac{H}{L} = 0.70 - 0.89\,\mathrm{e}^{-3.004 Fr_L} \tag{2}$$

$$\frac{K}{L} = 0.466 + 3.720\,\mathrm{e}^{-9.936 Fr_L} \tag{3}$$

for uniform debris and $0.10<Fr_L<0.51$.

The respective expressions for non-uniform debris are

$$\frac{W}{L} = 0.77 + 0.94\,\mathrm{e}^{-4.63 Fr_L} \tag{4}$$

$$\frac{H}{L} = 0.39 - 0.46\,\mathrm{e}^{-5.77 Fr_L} \tag{5}$$

$$\frac{K}{L} = 0.25 + 1.18\,\mathrm{e}^{-15.04 Fr_L} \tag{6}$$

for $0.10<Fr_L<0.40$.

2.2. *Estimating the size of the design log*

The results of field and laboratory observations show that the length of debris pieces is the among the most important variables determining the size of accumulations. As a result, the

methods described in the previous section for the evaluation of the size of debris jams at piers require the estimation of the length of the longest logs transported by the river (or simply the typical length of logs in uniform debris situations). Ideally, this estimation would be performed through detailed observations of the woody debris transported during flood events and of previous accumulations observed at piers. In addition, knowledge of the heights of riparian and floodplain vegetation can be helpful for inferring the maximum length of logs that can likely end up in the channel. In the absence of local information of the size of logs transported by the river, the methodology described by Diehl (1997) can be used, which recommends the smallest of: (*i*) the maximum length of sturdy logs, and (*ii*) the minimum width of the channel immediately upstream of the bridge[1]. The second condition takes into consideration that logs wider than channels are likely to jam between banks.

[1] Diehl (1997) specified a third condition to estimate the length of the log transported by the river, however, likely to be site-specific as referred to observed U.S. floating woody debris accumulations. That condition introduces the minimum width of the channel immediately upstream of the bridge as a third length at play.

3. ASSESSING THE EFFECTS OF DEBRIS JAMS ON PIER LOADINGS

Bridge piers located in flowing waters are subjected to both hydrodynamic and hydrostatic forces. The hydrostatic component results from differences in the flow depth at the upstream and downstream sides of the bridge. The hydrodynamic force, which is usually referred to as drag, results from the distribution of pressures on objects submerged in flowing fluids. For practical purposes, the total streamwise component of the hydraulic force exerted on a pier can be partitioned as such by the expression (Parola et al. 2000)

$$F_x = F_d + F_h \tag{7}$$

where F_x is the x- (streamwise) component of the total force (N), F_d is the drag force (N) and F_h is the net hydrostatic force (N), which is simply given by the difference in hydrostatic force exerted upstream and downstream of the object (F_h=F_{hu}-F_{hd}).

Because of the substantial increase in the obstructed area of flow that results from the accumulation of debris at piers, the drag component exerted on a pier can be considerably magnified by the formation of debris jams. The magnitude of the drag force is primarily a function of the geometry of the debris accumulation and can be assessed through the empirical drag equation

$$F_d = \frac{1}{2}\rho C_d A U^2 \tag{8}$$

where F_d is the drag force (N), ρ is the density of water (kg/m^3), C_d is the dimensionless coefficient of drag, A (m^2) is the projected area of the submerged object upon which the force is exerted and normal to the flow and U (m/s) is a reference velocity (typically the depth averaged approach flow velocity). In problems involving the accumulation of debris on piers, the drag force F_d can be partitioned into two components,

$$F_d = F_{dd} + F_{dp} \tag{9}$$

where F_{dd} is the drag exerted on the debris obstruction and F_{dp} the drag on the area of the pier underneath the debris jam [i.e. the area of pier is approximately given by A_p=(h-H)D, where h

is the depth of flow and D is the width of the pier or diameter for circular piers]. The blockage area of debris accumulations can be computed assuming the triangular projected shape of the half-conical debris accumulations $A_d=WH/2$ (where W and H can be estimated from the relations presented in the previous section – see **Figure 3**).

In general, the coefficient of drag, C_d, of submerged objects depends on several geometric and flow factors (e.g. the shape of the object, angle of attack, the Reynolds number, flow contraction, turbulence intensity and waves). Values of C_d of objects having well-defined geometry have been widely reported, which provide a relatively accurate estimate of drag exerted on many piers. For example, for cylindrical piers, the value of C_d=1.2 provides a good approximation over a wide range of the Reynolds number ($5x10^2$<Re<$1.2x10^5$) (Douglas et al. 2005), where Re=UD/ν, and ν (m^2/s) is the kinematic viscosity. However, debris accumulations display irregular shapes that pose important challenges to the accurate determination of C_d values. A number of studies have been conducted that can provide guidance on how to select the coefficient of drag of debris accumulations. These results are summarized in the **Table A**.

Table A. Summary of previous studies on the coefficient of drag of debris accumulations

Reference	Type of study	C_d values	Observations
Apelt (1986) (from Parola et al. 2000)	Experiments with idealised (rectangular perforated prism) models of debris accumulations	1.0~2.0	Results in absence of bridge piers or superstructure models
Wellwood and Fenwick (1990)		1.04	Approach flow velocity defined at mid-height of the debris accumulation
Parola et al. (2000)	Experiments with idealised (vertical plates, roughened cones on piers, roughened wedges) models of debris accumulations, as well as model debris	0.16~1.9	'Contracted' flow velocity used. Values of C_d have been observed to decrease with the blockage ratio (i.e. ratio between obstructed area and the total cross-sectional area)
Panici and de Almeida (2018) University of Southampton	Experiments with model debris (twigs and branches)	0.75~3.0	Most of the results within the narrower band of 1.0~2.5
AASHTO (1998) (from Parola et al. 2000)		0.1~1.8	Defined as a function of the blockage ratio and the Froude number
Shields and Gippel (1995)	Experiments using debris models of polyvinyl chloride (PVC) pipes and wooden dowels	1~2.5	Defined as a function of the blockage ratio and the drag coefficient of a cylinder of infinite length
Ontario Highway Bridge Design Code (1991) from AASHTO (2007)		1.4	Debris lodged against the pier
Draft of the New Zealand Highway Bridge Design Specification, from AASHTO (2007)		0.5	Defined as the drag coefficient of a floating debris accumulation of dimensions (triangular shape): -H = half of the water depth with 3 m maximum, and -W = half the sum of adjacent span lengths with 14 m maximum

Drag exerted by the pier on flow leads to afflux, as described in section 5. Where afflux is high, the difference between hydrostatic pressures up- and downstream of the pier will also produce additional loadings. A completely analytical treatment for the problem of determining the hydrostatic component of the force exerted on porous media such as debris jams has not been proposed in the literature. Simplified formulations are however available which model the forces on an idealised solid accumulation (Parola et al., 2000) as:

$$F_{hu} = \rho g h_{c-u} A_u \tag{10}$$

where F_{hu} is the hydrostatic force on the upstream side of the debris accumulation, A_u is the projected area of the submerged part of the accumulation normal to the flow direction, $h_{c\text{-}u}$ is the vertical distance from the free surface to the centroid of the area A_u. The same relation can be used to compute the downstream hydrostatic force F_{hd} from the corresponding values of A_d and $h_{c\text{-}d}$ on the downstream side of the jam. Assuming that the half-conical shape described in **Figure 3**, the cross-sectional areas A_u and A_d are triangular, and therefore $h_{c\text{-}u}=H/3$ and $h_{\text{c-d}}=(H-\Delta h)/3$ (where Δh is the afflux).

Other potential loadings on piers that result from the impact of wood debris are not dealt with in this guide.

4. ASSESSING THE INFLUENCE OF DEBRIS ON LOCAL SCOUR AT BRIDGE PIERS

Scour is the general term used to denote the phenomenon of lowering a channel bed elevation through the removal of sediment by the flow. Severe scour may undermine the foundations of bridge piers, a mechanism that has been widely recognised as the main cause for the collapse of bridges around the world. Depending on the mechanisms leading to its development, scour is classified as general, contraction or local scour. General and contraction types of scour occur due to a general modification of the flow features in the river and as a result of flow acceleration through the cross-sectional narrowing, respectively. Typically, these two types will lead to a generalised drop of the bed elevations across the channel. On the other hand, local scour is developed in the vicinity of instream structures as a result of the modification of the flow field that is produced by the structures obstruction.

Floating debris accumulations at bridge piers further complicate and magnify the phenomenon of local scour. The flow obstruction produced by debris jams induces an acceleration of the flow within the reduced depth of the fluid layer underneath the jam. The obstruction of the upper interface also prevents the flow field from forming a bow wave due to the stagnation pressure at the upstream face. The latter, along with the triangular longitudinal profile of the debris jams, forces the flow towards the bed producing a more intense erosive action (**Figure 5**).

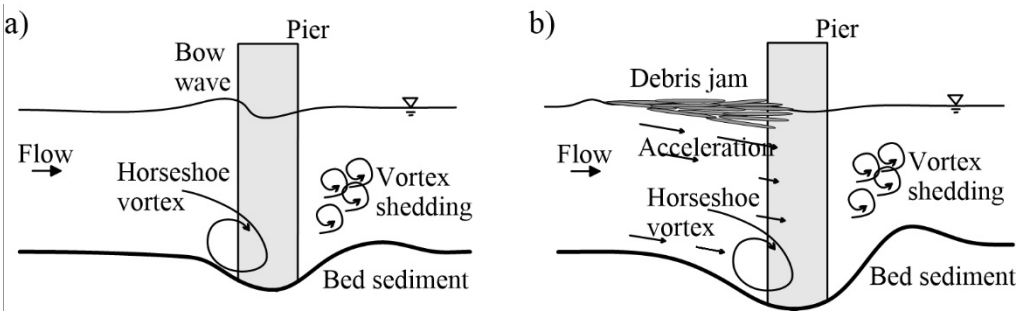


Figure 5. Sketch of the physics of the scouring process at piers: a) in the absence of debris, and b) affected by debris jams

This guide is exclusively concerned with the increase in the depth of local scour that results from the accumulation of floating debris at bridge piers. However, the next section provides a brief overview of other guides that can be consulted for the estimation of local scour at bridge piers without considering the effect of debris accumulations.

4.1. *Estimation of local scour in absence of debris jams*

The evolution of the scour depth at a bridge pier in absence of debris accumulation has been extensively studied over the decades and, thus, many empirical formulae are available in the literature to estimate the depth of local scour (Richardson and Davis, 1995; Dey, 1997; Melville and Chiew, 1999; Melville and Coleman, 2000; Sheppard and Miller, 2006; Sheppard et al., 2014). These methods are largely based on experiments and field measurements, restricting is applicability to the conditions similar to those for which they were formerly developed. Among them, the HEC-18 pier scour equation, based on the Colorado State University (CSU) equation, which describes the use of the Richardson and Davis's (1995) method, is the most used appraisal in bridge scour manuals around the world. **Table B** provides an overview of the main literature currently available on scour.

Table B. Summary of up-to-date bridge scour manuals

Reference	Title	Fundamental formulation
Sheppard and Renna (2005)	Bridge scour manual	Sheppard's formula
Arneson et al. (2012)	HEC-18 Evaluating scour at bridges	HEC-18 pier scour equation
Queensland Government (2013)	Bridge scour manual	HEC-18 pier scour equation
Kirby et al. (2015)	CIRIA's Manual on scour at bridges and other hydraulic structures	Breusers et al. (1977)'s equation

A complete, comprehensive guide on the evaluation and mitigation of the scour at bridge structures on rivers in UK and Ireland, is provided in CIRIA's "Manual on scour at bridges and other hydraulic structures" (Kirby et al. 2015, 2017). Note that CIRIA's guide was aimed at providing specific guidance within the contexts, regulations and legislation of the UK and the Republic of Ireland.

4.2. *Estimation of scour induced by debris jams*

Over the past decades, new research efforts have been devoted to understanding the effect of debris accumulations on local scour around bridge piers. These studies have provided design engineers with guidance on how to estimate scour for given characteristics of the accumulations. Most of the research in this field was based on laboratory experiments in which idealized models of debris accumulations (e.g. smooth, impermeable and regular shapes) were used. Guidance available on the potential increase in scour depth due to the presence of debris rafts varies considerably. For instance, according to the experiments of Melville and Dongol (1992), the maximum scour depth in presence of debris accumulation was 1.49 times larger than the scour depth without accumulation, whilst Pagliara and Carnacina (2010) found that debris increased scour by a factor of 2 to 3. In these studies, the dimensions and shape of models representing debris accumulations were initially assumed, and their influence on scour was tested in the laboratory. As scour depends strongly on the dimensions of the debris accumulations, the use of models that do not represent the size of debris jams that are likely to be formed under the corresponding experimental conditions may introduce an important source of uncertainty. This might explain the widely different results reported, although other characteristics of each experimental set up may also have played an important role. A few predictive methods have been proposed in the literature based on experimental data. One such methodology that has become popular is the computation of the so-called effective diameter (Melville and Dongol, 1992; Lagasse et al., 2010). The effective diameter is defined as an equivalent single-pier width which, in the absence of debris accumulation, would induce the same local scour that would develop in the presence of debris. This effective diameter is computed from the dimensions of the pier and debris accumulation as (Melville and Dongol, 1992):

$$D_e = \frac{T_d^* W + \left(h - T_d^*\right) D}{h} \tag{11}$$

where T^*_d=0.52H. Lagasse et al. (2010) found that this methodology tended to overestimate the depth of scour, and proposed a modified version of equation (11) that included additional empirical parameters, and as a result, displayed better agreement with their experimental data.

A recent study has been conducted at the University of Southampton to determine the potential increase in scour depth caused by debris accumulations. The main difference between these and previous experiments was the use of debris models with characteristics (e.g. flow-

dependent shape and dimensions) corresponding to the experiments of Panici and de Almeida (2017), previously presented in section **2.1**. **Figure 6** shows an example of a debris model used in these experiments and its impact on scour. The experiments were conducted within the range of Froude number $0.18<Fr<0.36$, using a 0.1 m diameter pier model with a sediment material with 1.4 mm median size diameter in a flume 23 m long, 1.38 m wide, and 0.6 m deep. **Figure 7** depicts a summary of the results obtained in these experiments, which showed that debris accumulations increased the depth of scour by a maximum factor ranging from 1.25~1.75.



Figure 6. Example of woody debris models used during the experiments conducted at the University of Southampton and its impact on scour.

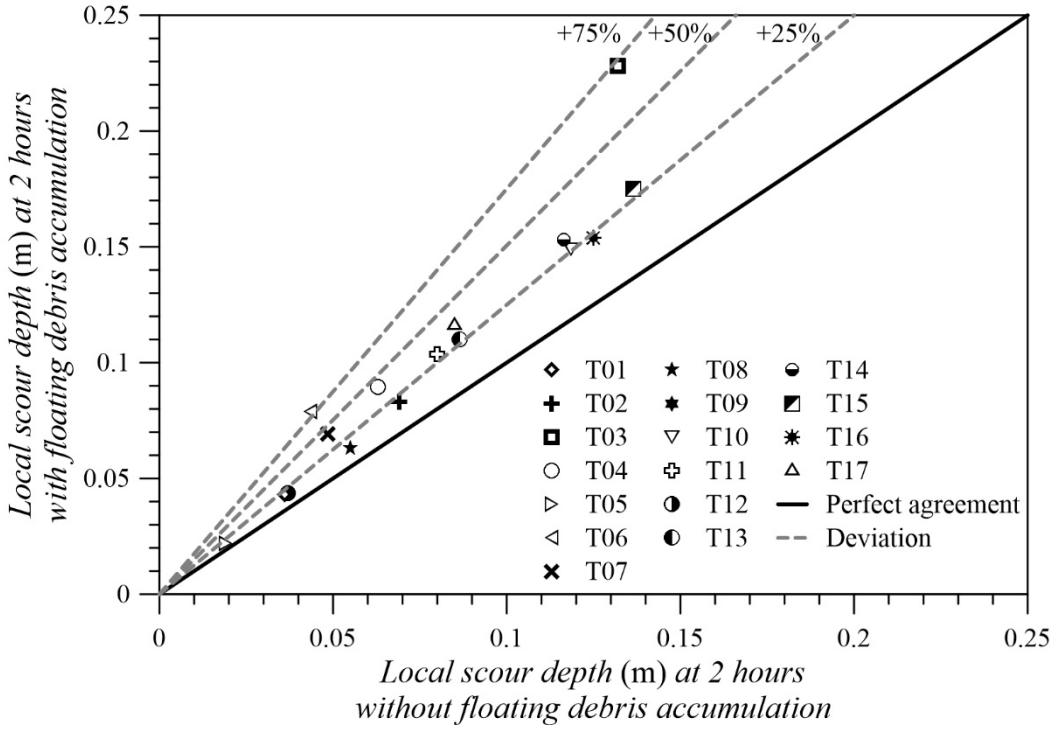


Figure 7. Comparison between local scour depth at 2 hours with and without floating debris accumulation using the experimental results produced for this booklet

The debris scour increase factors described above may be used as safety factors in engineering design when working to predict local scour depth. Whilst the 3-times factor from Pagliara and Carnacina (2010) may describe an extreme, worst-case scenario, the results from the University of Southampton suggest it may be overly conservative.

5. THE EFFECTS OF DEBRIS ON AFFLUX

5.1. *Understanding afflux*

The term *afflux* refers to an increase of the free surface level on the upstream side of a watercourse obstruction (e.g. a bridge pier) relative to the depth of the flow that would otherwise occur in the absence of the obstruction. Bridge piers submerged into flowing waters induce forces and energy losses that produce afflux. These effects can be considerably exacerbated when debris accumulates around a bridge pier. When drift jams extend across several spans and block a large proportion of the channel cross section, afflux can reach extreme levels.

The principles governing the phenomenon of afflux due to bodies submerged in open-channels —namely momentum (or alternatively energy) conservation— have been widely known for centuries. Over the past century, a few models have been proposed to estimate bridge pier afflux, either based on these first principles or completely empirically (Yarnell, 1936; El-Alty, 2006; Suribabu, 2011; Danish Hydraulic Institute, 2014; HEC-RAS River Analysis System, 2016). The widely acknowledged formula by Yarnell (1936), still recommended in many manuals, reads (HEC-RAS River Analysis System, 2016)

$$\Delta h = 2k\left(k+10\omega-0.6\right)\left(\alpha+15\alpha^4\right)\frac{U^2}{2g} \tag{12}$$

where k is the Yarnell's pier shape coefficients, ω is the ratio of velocity head to depth downstream the pier (or equivalently, ω=0.5Fr^2), α is the obstructed area of the pier divided by the total unobstructed area, and U is the reference velocity downstream the pier (refer **Figure 8**). Although similar from a theoretical point of view, less attention has been given to the development of tools to compute afflux in bridge piers affected by debris jams. Only a few studies have been conducted to date to empirically test the effects of debris jams on afflux, but they have been limited in scope and have not reached a level of accuracy required to be adopted in practical applications. In this guide we propose methods that are based on first principles (i.e. conservation of linear momentum) combined with empirical evidence to model the size and shape of accumulations (i.e. section 2.1) and the coefficient of drag of debris jams (e.g. section 2.2).

5.2. *Theoretical background*

The problem of afflux can be described on the basis of momentum conservation in a control volume of fluid between two cross sections. **Figure 8** shows a schematic profile of a typical river affected by an obstruction formed by the bridge pier and the debris accumulation. Under these conditions, the upstream water level needs to rise by a certain amount Δh (afflux) in order to balance the energy loss due to the drag force F_d exerted by the pier-debris on the fluid. In general, the friction force F_f exerted by the river bed on the fluid also introduces a variation of the normal depth h along the longitudinal axis. However, this backwater effect is typically small compared to the effect of the pier-debris drag, provided that the distance between sections A and B is short, so that the effect of F_f on the afflux can be neglected without much loss of accuracy.

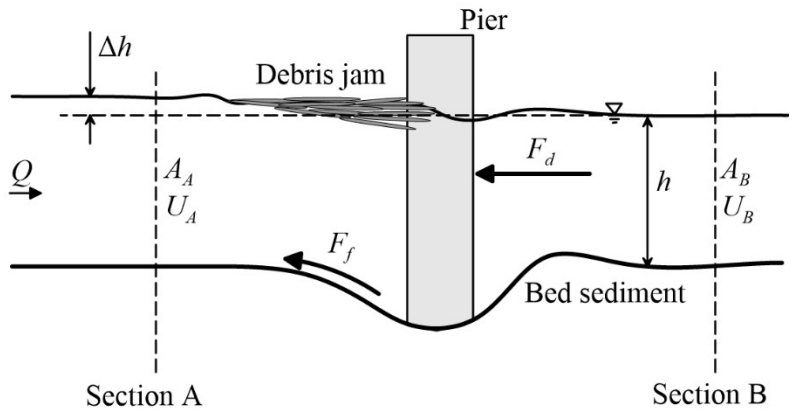


Figure 8. Schematic profile of a river in the vicinity of a bridge pier affected by debris accumulation.

Neglecting the component of the fluid's weight in the streamwise direction (i.e. assuming the slope between A and B is negligible) the application of the principle of momentum conservation in the streamwise direction to a prismatic one-dimensional (1D) open channel yields the well-known momentum equation:

$$F_{pA} - F_{pB} - F_x = \rho Q\left(U_B - U_A\right) \tag{13}$$

where F_{pA} and F_{pB} are the area-integrated hydrostatic forces on the upstream and downstream sections A and B respectively,

$$F_{pA} = \rho g h_{cA} A_A \tag{14}$$

$$F_{pB} = \rho g h_{cB} A_B \tag{15}$$

where A_A and A_B are the cross-sectional area in section A and B respectively, h_{cA} and h_{cB} are the vertical distances from the free surface to the centroid of the areas A_A and A_B respectively, and F_x is the total streamwise force exerted by the pier-debris on the flow [i.e. equation (7)]. Equations (14) and (15) depend on the shape of cross sections A and B, while F_x is a function of the properties of the debris accumulation and pier (dimensions and coefficient of drag). Solutions for the problem above have been implemented into a user-friendly software (*DEBRIS-Afflux Calculator v*1.0) for pier cross sections of particular shapes. The software computes the value of afflux from equation (13) by estimating the dimensions of wood debris jams as described in section 2 (Appendix B). Appendix C provides guidance on how to use the software.

6. REFERENCES

AASHTO. (1998). LRFD bridge design specifications, 2th Ed., Washington, DC.

AASHTO. (2007). LRFD bridge design specifications, 4th Ed., Washington, DC.

Aplet, C. J. (1986). "Flood forces on bridges." *Conference Proceedings, 13th AARB-5th REAAA Combined Conference*, Adelaide, Australia, 13 (6), 40-46.

Arneson, L. A., Zevenbergen, L. W., Lagasse, P. F., and Clopper, P. E. (2012). "Evaluating scour at bridges (HEC-18)." Technical Rep. No. FHWA (Federal Highway Administration) HIF-12-003, Washington, DC.

Benn J (2013) Railway bridge failure during flooding in the UK and Ireland. Proceedings of the Institution of Civil Engineers – Forensic Engineering 166(4): 163–170, http://dx.doi.org/10.1680/ feng.2013.166.4.163.

Bradley, J. B., Richards, D. L., and Bahner, C. D. (2005). "Debris control structures: Evaluation and countermeasures." Rep. No. FHWA-IF-04- 016, U.S. DOT, Federal Highway Administration, Washington, DC.

Breusers, H. N. C., Nicollet, G., and Shen, H. W. (1977). "Local scour around cylindrical piers." *J. Hydraul. Res*., 15(3), 211–252.

Cook, W. (2014). "Bridge failure rates, consequences, and predictive trends." Ph.D. thesis, Utah State Univ., Logan, UT.

Danish Hydraulic Institute (2017). MIKE11: a modelling system for rivers and channels. User guide.Dey, S. (1997). "Local scour at piers, Part I: A review of developments of research." Int. J. Sediment Res., 12(2), 23–46.

Dey, S. (2014). Fluvial hydrodynamics: Hydrodynamic and sediment transport phenomena, Springer, Berlin.

Diehl, T. H. (1997). "Potential drift accumulation at bridges." U.S. Dept. of Transportation, Federal Highway Administration, Rep. FHWA-RD-97- 028, Washington, DC

Douglas, J. F., Gasiorek, J. M., Swaffield, J. A., and Lynne, B. J. (2005). Fluid mechanics, Harlow, England.

El-Alfy, K. S. (2006). "Experimental study of backwater rise due to bridge piers as flow obstructions." Tenth International Water Technology Conference, IWTC 10,2006, 319-336.

Harada, N., Nakatani, K., Satofuka, Y., and Mizuyama, T. (2017). "Traditional technique in Japan to prevent bridge blockages caused by driftwood using stakes." Proceedings of the 37th IAHR World Congress, Kuala Lumpur, Malaysia.

HEC-RAS River Analysis System (2016). Hydraulic Reference Manual, US Army Corps of Engineers, Hydrologic Engineering Center.

JBA CONSULTING. Afflux Advisor User Manual. Department for Environment, Food and Rural Affairs/Environment Agency, UK, 2005, R&D Project W5A-065.

Kirby, A., Roca, M., Kitchen, A., Escarameia, M., and Chesterton, O. (2015). Manual on scour at bridges and other hydraulic structures, CIRIA.

Lagasse, P. F., Clopper, P. E., Zevenbergen, L. W., Spitz, W. J., and Girard, L. G. (2010). "Effects of debris on bridge pier scour." NCHRP Rep. 653, Transportation Research Board, National Academies of Science, Washington, DC.

Lyn, D., T. Cooper, D. Condon, and L. Gan (2007). Factors in debris accumulation at bridge piers, Washington, U.S. Dept. of Transportation, Federal Highway Administration Research and Development, TurnerFairbank Highway Research Center, McLean, Va.

Manners, R. B., Doyle, M. W., and Small, M. J. (2007). "Structure and hydraulics of natural woody debris jams." Water Resour. Res. 43(6), W06432.

Melville, B. W., and Chiew, Y.-M. (1999). ''Time scale for local scour at bridge piers.'' J. Hydraul. Eng., 125(1), 59–65.

Melville, B. W., and Coleman, S. E. (2000). Bridge scour, Water Resources, Fort Collins, Colo.

Melville, B. W., and Dongol, D. M. S. (1992). "Bridge scour with debris accumulation." J. Hydr. Engrg., ASCE, 118(9), 1306-1310.

Ontario Ministry of Transportation. (1991). Ontario highway bridge design code, Ottawa.

Pagliara, S. and Carnacina, I. (2011). "Influence of large woody debris on sediment scour at bridge piers." International Journal of Sediment Research, Vol. 26, No. 2, pp. 121-136.

Panici, D., and de Almeida, G. A. (2018). "Formation, growth and failure of debris jams at bridge piers." *Water Resources Research*.

Parola, A. C., Apeldt, C. J., and Jempson, M. A. (2000). "Debris forces on highway bridges." *National Cooperative Highway Research Program (NCHRP) Rep. No. 445*, Transportation Research Board, National Research Council, Washington, DC.

Queensland Government (2013). Bridge scour manual, Department of Transport and Main Roads, Queensland, Australia.

Richardson, E. V., and Davis, S. R. (1995). Evaluating scour at bridges: Federal Highway Administration Hydraulic Engineering Circular No. 18. Publication FHWA-IP-90-017.

Richardson, E. V., and Davis, S. R. 2001. "Evaluating scour at bridges." Hydraulic Engineering Circular No. 18, FHWA NHI 01-001, 4th Ed., US DOT, Washington, D.C.

Rusyda, M.I., Hashimoto, H., and Ikematsu, S., (2014). "Log jam formation by an obstruction in a river." Proc. Fluvial Hydraul. RIVER FLOW 2014, 717–724.

Schmocker, L., and Weitbrecht, V. (2013). "Driftwood: risk analysis and engineering measures." J Hydraul Eng 139(7):683–695.

Sheppard, D. M., and Renna, R. (2005). Bridge scour manual, Florida Department of Transportation, 605.

Sheppard, D. M., and Miller, W. (2006). "Live-bed local scour experiments." J. Hydraul. Eng., 132(7), 635–642.

Sheppard, D. M., Melville, B., Demir, H. (2014). “Evaluation of existing equations for local scour at bridge piers.” J Hydraul Eng 140(1):14–23

Shields. F. D. Jr.. and Gippel. C. J. (1995). "Prediction of effects of woody debris removal on flow resistance." J. Hydr. Engrg.. ASCE. 121(4).341-354.

Suribabu, C.R., Sabarish, R.M., Narasimhan, R.E. and Chandhru, A.R. (2001) "Backwater rise and drag characteristics of bridge piers under subcritical flow conditions", European Water, 36(1): 27-35.

Szydłowski, M. (2011). “Numerical simulation of open channel flow between bridge piers.” *TASK Quarterly*, *15*(3-4).

Wallerstein, N. P., Thorne, C. R., and Abt, S. R. (1996). “Debris control at hydraulic structures—Management of woody debris in natural channels and at hydraulic structures.” Rep. Prepared for the U.S. Army Corps of Engineers, Waterways Experiment Station, Vicksburg, MS.

Wellwood, N. and Fenwick, J. (1990). “A flood loading methodology for bridges”, *Conference Proceedings, 15th ARRB Conference*, 3:315–341.

APPENDIX A: CASE STUDY ILLUSTRATING THE ASSESSMENT OF THE BRIDGE PIER SCOUR

This appendix contains a case study illustrating the proposed assessment of potential local scour depth at bridge piers in presence of debris accumulation.

A1. Llangadog viaduct. River Sawdde, Llangadog, Wales, UK.

The case study A1 is based on the detailed scour assessment report of the Network Rail *VOT – 23 33.5* bridge by JBA consulting in March 2010. The *VOT – 23 33.5* bridge is located 7 km to the south west of Llandovery, Wales (Figure A1).

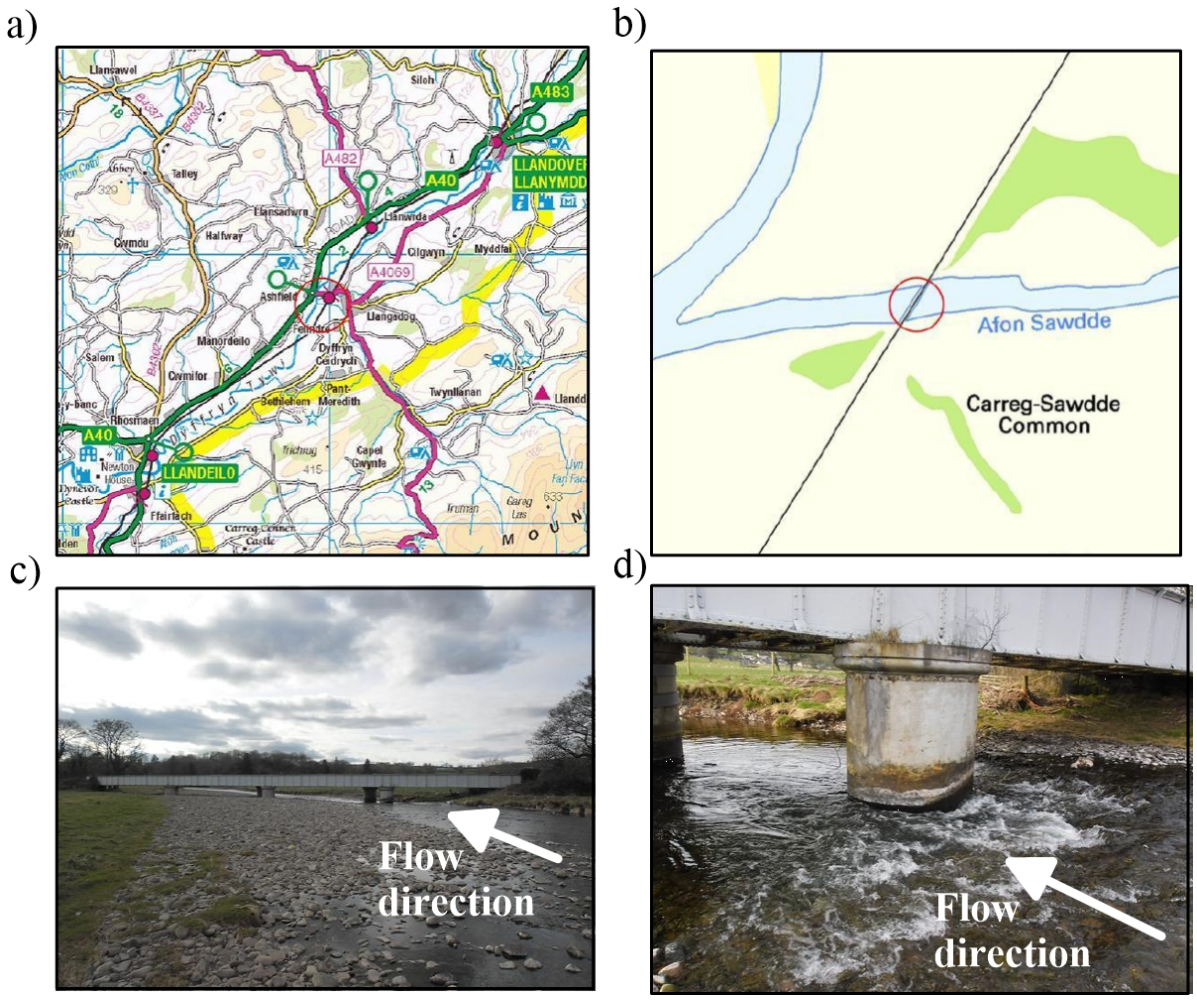


Figure A1. Location plans and photograph of the assessed bridge pier: (a) 1:200.000, (b) 1:5.000, (c) general photograph, and (d) detail photograph. Contains Ordnance Survey data © Crown copyright and database right 2018

The structure of the bridge consists of a four-span steel deck supported on masonry abutments and steel piers on the River Sawdde. The piers consist of paired steel columns

oriented to the main direction of the flow. According to JBA, the foundation base of the piers was assumed to be 3m below the bed sediment level.

In the risk assessment conducted by JBA consulting, the design flood, water levels and velocities were computed by using several manuals and commercial software. Namely, the Flood Estimation Handbook (Reed et al., 1999) and the Flood Estimation Software v2.0 (JBA Consulting, 2007) were employed for estimating the design flood, whilst the water levels and velocities were estimated by using HEC-RAS model. The result of these calculations is summarized in Table A1 at different return periods of flood.

Table A1. Design floods, water levels and velocities by JBA Consulting (2013)

Return period	2-year	5-year	10-year	25-year	50-year	100-year	150-year	200-year
***Design flood* (m^3/s)**	252.37	312.04	353.06	409.74	456.50	507.66	539.96	564.02
***Water level above datum* (mAD)**	10.22	10.47	10.69	10.95	11.16	11.27	11.99	12.03
***Average channel velocity* (m/s)**	2.21	2.62	2.96	3.44	3.83	4.33	2.76	2.79

For our illustrative purpose, the depth of local scour was estimated using the Breusers et al. (1977) method by CIRIA's *Manual on scour at bridges and other hydraulics structures* (Kirby et al. 2015, as follows.

$$\frac{y_s}{D} = \Phi_{shape}\Phi_{depth}\Phi_{velocity}\Phi_{angle} \tag{16}$$

Φ_{shape}, Φ_{depth}, $\Phi_{velocity}$ and Φ_{angle} are factors accounting for the effect of shape, flow depth, velocity and angle at piers, respectively. The values of the coefficients Φ_{shape}=1.5 (circular pier), Φ_{angle}=1.0 (circular pier), $\Phi_{velocity}$=1.0 (i.e. worst-case scenario, assumed in the absence of sediment grain size data needed to compute the threshold velocity) and Φ_{depth}=1.0 (assuming that h/D>2.7) are assumed here. A more detailed assessment would need to be conducted for each individual pier based on local values of velocities and depth, but this is outside the objective of this illustrative example. Using the above values, along with a safety factor SF=1.6, results in y_s/D=2.4.

The assessment of the effect of debris on local scour depth at the bridge piers can now be performed using the information provided by this guide following two approaches recommended in CIRIA's manual: (i) using Φ_{debris}=1.75 as the maximum effect, as reported by the experiments conducted at University of Southampton (section 4.2), and (ii) calculating the effective pier diameter from the dimensions of the potential debris accumulation (i.e. section 2.1). The first approach is a straightforward implementation in Breusers et al.'s (1977) formula and results in y_s/D=4.2. The second approach, however, requires knowledge of the length L of the longest logs likely to be transported in the river. Unfortunately, no vegetation survey in the River Sawdde catchmentat Llangadog could be consulted by the time this guide was written. To provide an illustrative example of the application of the second approach, the length of the longest log is estimated based on a visual inspection using site pictures. According to the Diehl's (1997) methodology described in section 2.2, it is assumed that the maximum length of sturdy logs is 12m while the minimum width of the channel immediately upstream of the bridge is approximately 20m. This approximation leads to L=12m, which can be inserted into equations (4)-(6) to estimate H, W, and K for the potential debris accumulation and, hence, the effective pier diameter using equation (11). The results are summarized in Table A2.

Table A2. Average debris-induced local scour depth at piers in the Network Rail *VOT – 23 33.5* bridge using methodology given in this guide

Piers	**Average local scour (m)**
By this guide using F_{debris}=1.75	9.77
By this guide using D_e	8.93

Note: Using CIRIA's manual, the pier diameter was computed as D=2.5m. Therefore, the 200-year return period with L=12m led to H=3.42m, W=12.67m, K=3.29m, and D_e=4m.

APPENDIX B: MATHEMATICAL RELATIONS USED TO COMPUTE AFFLUX (*DEBRIS-Afflux Calculator v*1.0)

As briefly described in previous sections of this manual, the *DEBRIS-Afflux Calculator v*1.0 software computes the afflux by solving the one-dimensional momentum equation (i.e. equation 13). The software implements solutions to this equation for two cross-sectional shapes that are of practical interest in engineering: (i) trapezoidal cross-sectional open channels, and (ii) compound open channels. The mathematical relations used to compute afflux for prismatic trapezoidal channels are detailed below. In both cases, *DEBRIS-Afflux Calculator v*1.0 computes the projected blockage area A_b using the same formulation. Here we present the relations used to compute afflux for the problem of a trapezoidal section only. The corresponding relations for compound channels are based on the same approach (momentum conservation) but result in more complex formulations that are not shown in this guide for brevity.

Assuming that the cross-section of half-cone shape of the woody jam depicted in **Figure 3** is symmetric about the pier axis, A_b can be determined by as

$$A_b = \frac{1}{2}HW + (h-H)D + \frac{HD^2}{2W} \tag{17}$$

Note that the first, second and third terms in the right-hand side of equation (17) correspond to the projected area of the floating debris accumulation, the cylindrical piece of pier below the debris, and area of the cylindrical pier above the lowest point of the accumulation, respectively.

Likewise, the upstream and downstream hydrostatic forces on the debris accumulation are given by

$$F_{hu} = \rho g W \frac{H^2}{6} \tag{18}$$

$$F_{hd} = \rho g W \frac{(H-\Delta h)^3}{6H} \tag{19}$$

Trapezoidal cross-sectional open channels

Using equation (13), the momentum balance applied to a control volume in the vicinity of a debris-pier obstruction is given by

$$F_{pA} - F_{pB} - \rho g \frac{W}{6}\left[H^2 - \frac{\left(H-\Delta h\right)^3}{H}\right] - \frac{1}{2}\rho\left(\frac{Q}{A_A}\right)^2\left(C_{dd}A_d + C_{dp}A_p\right) = \rho\left(\frac{Q^2}{A_B} - \frac{Q^2}{A_A}\right) \quad (20)$$

where A_A and A_B are the cross-sectional areas in sections A and B, respectively. Considering a flow of constant density in a prismatic, trapezoidal channel cross-sectional with symmetrical bank slopes S_b, the hydrostatic pressure at sections A and B are, respectively

$$F_{pA} = \rho g \frac{\left(h+\Delta h\right)^2}{6}\left[3b + 2S_b\left(h+\Delta h\right)\right] \quad (21)$$

$$F_{pB} = \rho g\left(\frac{bh^2}{2} + \frac{h^3 S_b}{3}\right) \quad (22)$$

Inserting equations (21)-(22) into equation (20) yields

$$g\frac{\left(h+\Delta h\right)^2}{6}\left[3b + 2S_b\left(h+\Delta h\right)\right] - g\left(\frac{bh^2}{2} + \frac{h^3 S_b}{3}\right) - g\frac{W}{6}\left[H^2 - \frac{\left(H-\Delta h\right)^3}{H}\right] - \frac{1}{2}\left(\frac{Q}{A_A}\right)^2\left(C_{dd}A_d + C_{dp}A_p\right) = \left(\frac{Q^2}{A_B} - \frac{Q^2}{A_A}\right) \quad (23)$$

Equation (23) is iteratively solved by *DEBRIS-Afflux Calculator v*1.0 when the user selects a trapezoidal cross-sectional channel for computation.

APPENDIX C: *DEBRIS-Afflux Calculator v*1.0

The *DEBRIS-Afflux Calculator v*1.0 is a 1D model for assessing afflux in prismatic single and compound channels using a momentum balance in a control volume that includes the pier-debris obstruction. The software allows users to assess flow produced by obstructions formed by single pier bridges and debris accumulation, where the pier is located in the cross-section of the main channel. The physics of the problem, as well as the proposed mathematical model, were described in section 5.2 and **APPENDIX B:** MATHEMATICAL RELATIONS USED TO COMPUTE AFFLUX (*DEBRIS-Afflux Calculator v*1.0 of the present booklet). **Figure C1** shows a screenshot of the user interface by *DEBRIS-Afflux Calculator v*1.0.

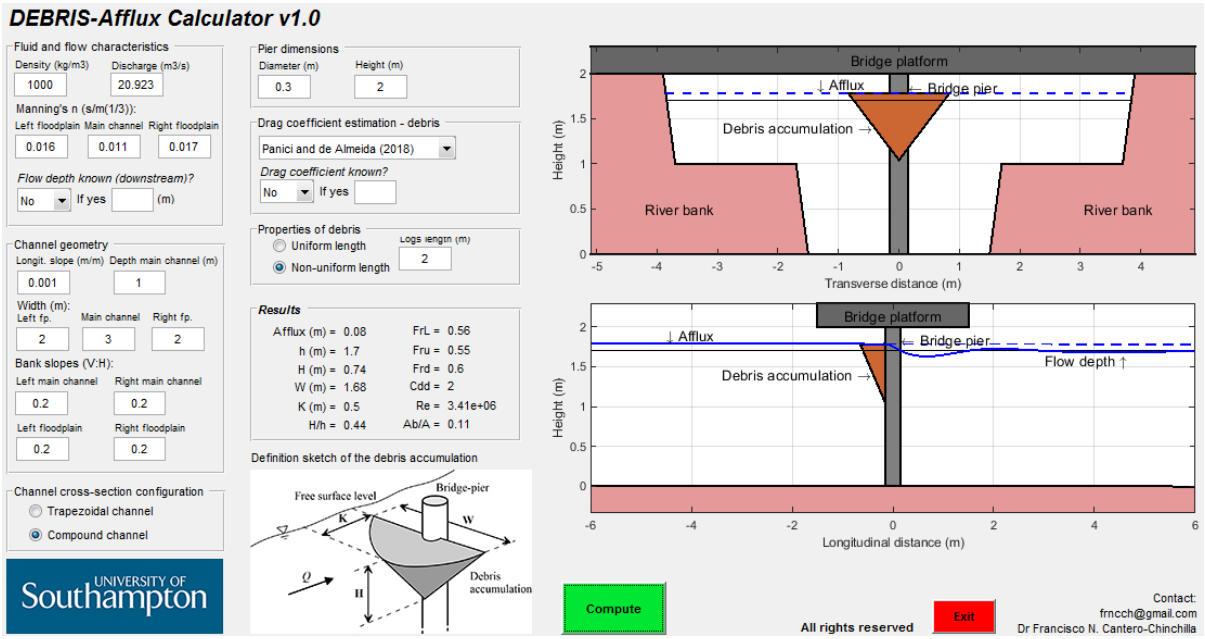


Figure C1. Screenshot of the *DEBRIS-Afflux Calculator v*1.0 for the compound channel configuration

The inputs to the model are divided in six main boxes, which need to be populated with information regarding (i) Fluid and flow characteristics, (ii) Channel geometry, (iii) Properties of debris, (iv) Channel cross-section configuration, (v) Pier dimensions, and (vi) Drag coefficient formula. The variables shown on the box 'Results' can be computed by clicking on the 'Compute' button. Finally, when the results are obtained, the user can finish using *DEBRIS-Afflux Calculator v*1.0 by clicking on '*Exit*'.

The software allows users to assess a wide range of scenarios of single pier and debris obstructions including, for instance: (i) no-debris obstruction by reducing the length of the key log to zero, and (ii) bridges having 2 piers by evaluating a symmetrical cross-sectional portion of the whole. Care must be taken in performing the analysis (ii) above. When two piers are

relatively close and there is a risk of span blockage (i.e. one log bridging the gap between two accumulations), the formulations presented in section 2.1 are not valid.

The entry of data into the user interface of the model is organized by frames as it is explained below.

i. Fluid and flow characteristics

Each of the variables in the '*Fluid and flow characteristics*' frame (as shown in **Figure C2**) are explained below.

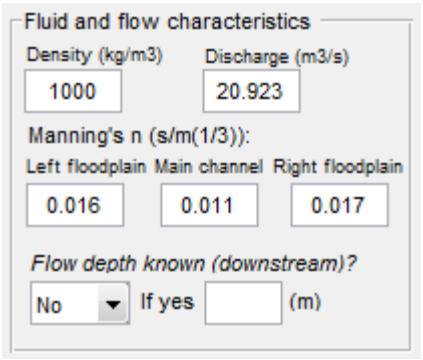


Figure C2. Fluid and flow characteristics frame for user-edition in *DEBRIS-Afflux Calculator v*1.0

- *Fluid density* (kg/m^3);
- *Discharge* (m^3/s);
- *Manning's coefficient for the main channel* (s/m$^{1/3}$);
- *Manning's coefficient for the left floodplain* (s/m$^{1/3}$); and
- *Manning's coefficient for the right floodplain* (s/m$^{1/3}$).

Further, the user is allowed to insert a direct estimation of the flow depth downstream of the pier if this value is known. A pop-up menu offers 'Yes' and 'No' options. If the option 'Yes' is selected, the model reads the value of the depth from text box on the right. If the depth is not known, the model adopts the uniform flow depth, which is computed with Manning's equation and the user-defined values of the channel's cross-section characteristics and slope.

When the user is assessing a trapezoidal channel, information of the Manning's in the left and right floodplain in **Figure C2** is not used. The numerical values entered in the *Fluid and flow characteristics* frame must be real and positive.

ii. Channel cross-section configuration

The computation of the afflux is performed in *DEBRIS-Afflux Calculator v*1.0 for trapezoidal or compound channel geometries. The governing equations for the calculation of the afflux in trapezoidal channels has been shown in the previous section 5.2 and **APPENDIX B**, where equation (26) is implicitly solved using the Matlab ® function *vpasolve*. The software computes the normal flow depth by using the Manning formula for steady uniform flows. The governing equations for compound channels are not shown in the present booklet for the space sake. The model uses the vertical division method (Chow 1959, Cantero et al. 2015) for the computations in compound channels.

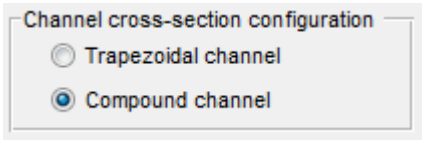


Figure C3. Channel cross-section configuration frame.

In the *Channel cross-section configuration* frame, the user can choose between (i) a trapezoidal channel or (ii) a compound channel.

iii. Cross-sectional channel geometry

The relevant channel geometry characteristics in the *DEBRIS-Afflux Calculator v*1.0 model can be edited in the '*Channel geometry*' frame of the user interface as shown in **Figure C4**.

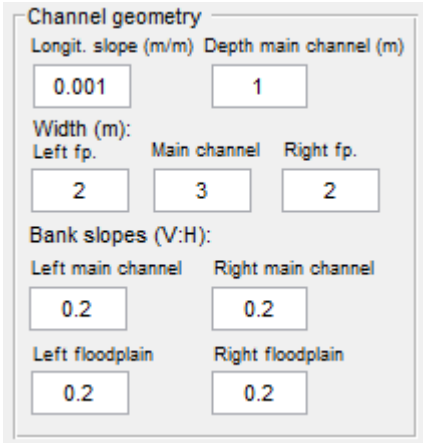


Figure C4. Channel geometry frame .

The variables in the *Channel geometry* frame are:

- *Width of the main channel* (m);
- *Width of the left floodplain (without the banks' slope)* (m);
- *Width of the right floodplain (without the banks' slope)* (m);

- *Longitudinal slope* (m/m);
- *Slope of the left bank in the main channel* (vert:horiz; m/m);
- *Slope of the right bank in the main channel* (vert:horiz; m/m);
- *Slope of the bank in the left floodplain* (vert:horiz; m/m);
- *Slope of the bank in the right floodplain* (vert:horiz; m/m); and
- *Depth of the main channel* (m).

When a trapezoidal channel is chosen, the width and bank slope of the left and right floodplain are not used by the model. All numerical values entered in the data in the Channel geometry frame must be real and positive.

iv. Properties of debris

The properties of the floating debris transported by the river can be input into the model in the '*Type of debris*' frame, which is shown in **Figure C5**.

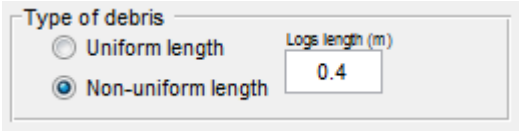


Figure C5. Properties of debris frame.

In the *Type of debris* frame, the user is allowed to choose between (i) uniform length or (ii) non-uniform length of debris. The first alternative is to be used when floating debris transported in the river has a uniform length, in which case the model uses equations (1)-(3) to compute the dimensions of the accumulations. The second option should be used to model debris formed by pieces that are non-uniformly distributed (most commonly observed in natural streams), which is modelled using equations (4)-(6). Further, the *Length of the key log* (m) value shown in **Figure C5** can be assessed as described in section 2.2 and must be real and positive.

v. Pier dimensions

Users can define the pier dimensions through the '*Pier dimensions*' frame in the user interface as shown in **Figure C6**.



Figure C6. Pier dimensions frame.

Note that the height of the pier is not used in the internal calculations by *DEBRIS-Afflux Calculator v*1.0, and only for adjusting the top of the plot. The variables in *Pier dimensions* frame are:

- *Diameter of the pier* (m); and
- *Maximum height of the pier* (m).

Note that the bridge platform is supposed to be resting on top of the pier. A bridge platform section of arbitrary dimensions is plotted on top of the pier for illustrative purposes only. All numerical values in the *Pier dimensions* frame must be real and positive.

vi. Drag coefficient formula

The drag coefficient can be modified by the user according to **Table *A*** as shown in the '*Drag coefficient formula*' frame in **Figure C7**. The model approximates the drag coefficient of a cylinder as follows:

$$C_d = \begin{cases} \dfrac{3.2}{\mathrm{Re}^{0.15}} & \text{if} \quad \mathrm{Re} < 10^3 \\ 0.13\,\mathrm{Re}^{0.2} & \text{if} \quad 10^3 < \mathrm{Re} < 10^4 \\ 1.2 & \text{if} \quad 10^4 < \mathrm{Re} < 1.5\cdot 10^5 \\ \dfrac{3\cdot 10^6}{\mathrm{Re}^{1.2}} & \text{if} \quad 1.5\cdot 10^5 < \mathrm{Re} < 4.5\cdot 10^5 \\ 0.003\,\mathrm{Re}^{0.3} & \text{if} \quad \mathrm{Re} > 4.5\cdot 10^5 \end{cases} \tag{24}$$

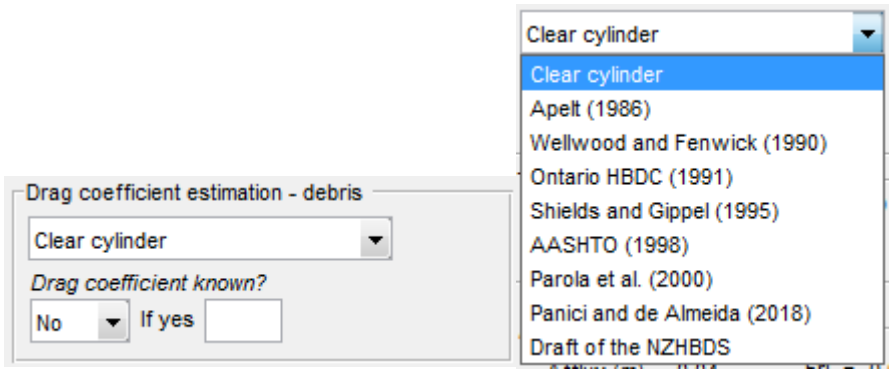


Figure C7. Drag coefficient formula frame.

Users can insert a direct estimation of the drag coefficient instead of using an option by **Table *A***. A pop-up menu offers 'Yes' and 'No' options. When the option 'Yes' is chosen, the model reads the value of C_d from text box at the right.

vii. Results frame

The variables shown in the Results frame (**Figure C8**) are explained below (some of them repeated here for convenience):

- *Afflux* = Δh = the increase in the upstream water level of a river channel caused by the presence of the pier and debris jam. (m);
- h = flow depth downstream of the pier(m).
- H = debris accumulation height (m);
- W = debris accumulation width (m);
- K = debris accumulation length in the streamwise direction (m);
- H/h = depth ratio (-);
- FrL = Froude number of logs (-);
- Fru = Froude number upstream the obstruction location (-);
- Frd = Froude number downstream the obstruction location (-);
- C_d = drag coefficient (-);
- Re = Reynolds number (-); and
- $A_b/A = A^*$ = blockage area ratio (-).

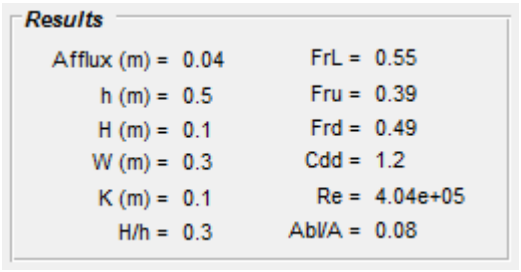


Figure C8. Results frame.

viii. Plots

The results are graphically displayed in the right-hand figures of the graphical user interface. These allow users to visualise the channel cross-sectional geometry, pier dimensions, as well as the size of the debris accumulation and afflux computed by the model. The debris accumulation is plotted at the free surface only for illustrative purposes. To help the user identify the elements in the plots, several labels are displayed in these figures.

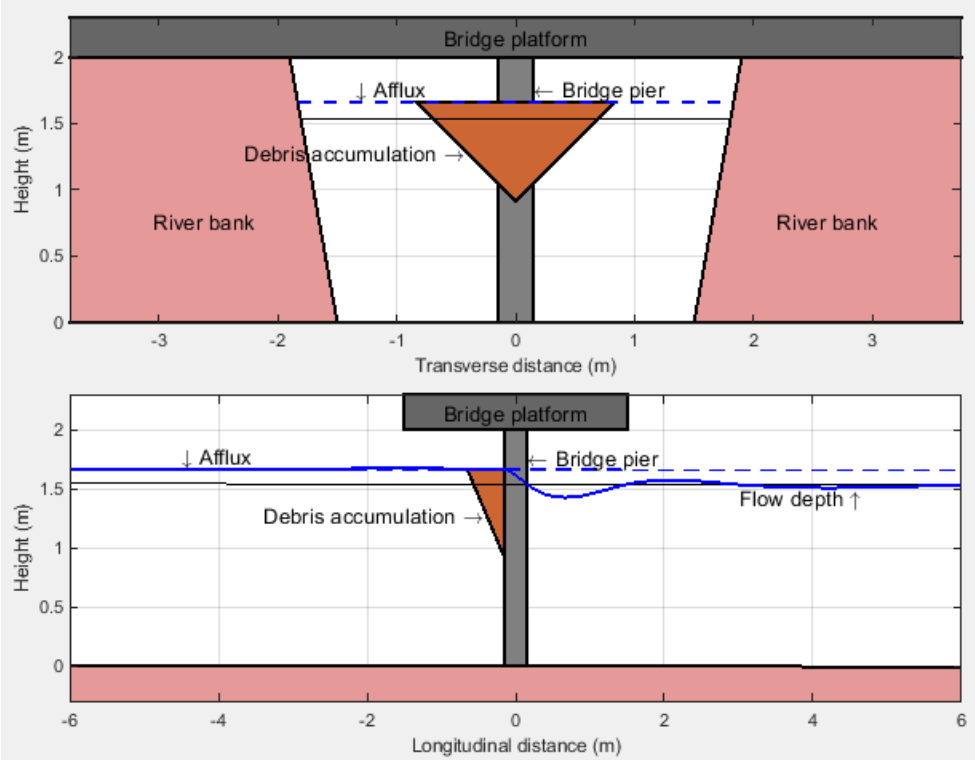


Figure C9. Plots frame in *DEBRIS-Afflux Calculator v*1.0

The results displayed in the figures are not editable.

ix. Warnings and Errors

A number of warnings and errors pop-ups have been coded to alert users of potential misuse of the software or about the some of the limitations of the model, as listed below.

Table C. List of messages, warnings and errors in *DEBRIS-Afflux Calculator v*1.0

No	Type	Comments	Action required
1	Disclaimer	See pg. 3.	Click on OK to accept.
2	Warning	*Transcritical flow*. Flow transients from supercritical to subcritical from one to the other side of the obstruction. The results may not be accurate since only subcritical flow conditions should be modelled with the software.	Click on OK to accept. Compute under subcritical flow conditions.
3	Warning	*Supercritical flow*. The flow is supercritical in the river. The results may not be accurate since only subcritical flow conditions should be modelled with the software.	Click on OK to accept. Compute under subcritical flow conditions.
4	Warning	Height of debris accumulation (H) is greater than the flow depth downstream the pier (h). The results may not be representative. A different calculation is encouraged to be performed.	Click on OK to accept. Provide settings to satisfy $h>H$.

5	Warning	The ratio W/B is out the range under the accumulation size equations where developed in laboratory (for non-uniform debris). It is $0.2<W/B<0.8$. Note that B is the width of the free surface.	Click on OK to accept. Provide settings to satisfy $0.2<W/B<0.8$.
6	Warning	The ratio W/B is out the range under the accumulation size equations where developed in laboratory (for uniform debris). It is $0.22<W/B<0.75$. Note that B is the width of the free surface.	Click on OK to accept. Provide settings to satisfy $0.22<W/B<0.75$.
7	Warning	The ratio H/B is out the range under the accumulation size equations where developed in laboratory (for non-uniform debris). It is $0.01<H/B<0.2$. Note that B is the width of the free surface.	Click on OK to accept. Provide settings to satisfy $0.01<H/B<0.2$.
8	Warning	The ratio H/B is out the range under the accumulation size equations where developed in laboratory (for uniform debris). It is $0.01<H/B<0.15$. Note that B is the width of the free surface.	Click on OK to accept. Provide settings to satisfy $0.01<H/B<0.15$.
9	Warning	The ratio K/B is out the range under the accumulation size equations where developed in laboratory (for non-uniform debris). It is $0.04<K/B<0.35$. Note that B is the width of the free surface.	Click on OK to accept. Provide settings to satisfy $0.04<K/B<0.35$.
10	Warning	The ratio K/B is out the range under the accumulation size equations where developed in laboratory (for uniform debris). It is $0.06<K/B<0.5$. Note that B is the width of the free surface.	Click on OK to accept. Provide settings to satisfy $0.06<K/B<0.5$.
11	Warning	The ratio L/D is out the range under the accumulation size equations where developed in laboratory (for non-uniform debris). It is $5<L/D<30$.	Click on OK to accept. Provide settings to satisfy $5<L/D<30$.
12	Warning	The ratio L/D is out the range under the accumulation size equations where developed in laboratory (for uniform debris). It is $3.75<L/D<15$.	Click on OK to accept. Provide settings to satisfy $3.75<L/D<15$.
13	Warning	Fr_L is out the range under the accumulation size equations where developed in laboratory (for non-uniform debris). It is $0.1< \mathrm{Fr}_L<0.5$.	Click on OK to accept. Provide settings to satisfy $0.1< \mathrm{Fr}_L<0.5$.
14	Warning	Fr_L is out the range under the accumulation size equations where developed in laboratory (for non-uniform debris). It is $0.1< \mathrm{Fr}_L<0.4$.	Click on OK to accept. Provide settings to satisfy $0.1< \mathrm{Fr}_L<0.4$.
15	Warning	Fr_u is out the range under the accumulation size equations where developed in laboratory. It is $0.104< \mathrm{Fr}_u<0.517$.	Click on OK to accept. Provide settings to satisfy $0.104< \mathrm{Fr}_u<0.517$.

16	Warning	The ratio H/h is out the range under the accumulation size equations where developed in laboratory. It is $0.071< H/h<0.703$.	Click on OK to accept. Provide settings to satisfy $0.071< H/h<0.703$.
17	Error	The drag coefficient is calculated following Shield and Gippel (1995) and the blockage ratio does not satisfy $0.03<A^*<0.3$ as the applicable range for using Shield and Gippel's formulation.	Click on OK to accept. Provide settings to satisfy $0.03<A^*<0.3$.
18	Error	Empty data.	Click on OK to accept. Provide a real and positive number.
19	Error	Known flow depth text box is blank. Uniform flow has been assumed to allow the calculation.	Click on OK to accept. If check box reads "Yes", provide a real and positive number.
20	Error	Drag coefficient error. Out of the definition range by ASSHTO (1998). C_{dd}=1.2 for a clear cylinder has been assumed to allow the calculation. Please, repeat the computation within the definition bounds.	Click on OK to accept. Provide settings to satisfy variable ranges as given in table 1 by ASSHTO (1998).

APPENDIX D: GLOSSARY OF TERMS AND ABBREVIATIONS

The following terms and abbreviations are used in this booklet:

- A_A = cross-sectional area at section A (m^2);
- A_B = cross-sectional area at section B (m^2);
- A_b = blockage area of the debris-pier obstruction (m^2);
- $A_b/A = A^*$ = blockage area ratio (-);
- A_d = projected area of the debris accumulation (on a plane perpendicular the main flow direction) (m^2);
- *Afflux* = Δh = the increase in the upstream water level of a river channel caused by the presence of the pier and debris jam (m);
- A_p = projected area of the pier (m^2);
- A_u = projected area of the submerged part upstream of the accumulation normal to the flow direction (m^2);
- C_{dd} = drag coefficient of the debris (-);
- C_{dp} = drag coefficient of the pier (-);
- D = pier diameter (m);
- D_e = effective diameter of the pier when debris is present (m);
- F_d = drag force (N);
- F_{dd} = drag exerted on the debris obstruction (N);
- F_{debris} = debris accumulation factor (-);
- F_{dp} = drag force exerted on the area of the pier below the debris jam (N);
- F_h = net hydrostatic force (N);
- F_{hd} = hydrostatic force exerted on the downstream side of the debris accumulation (N);
- F_{hu} = hydrostatic force exerted on the upstream side of the debris accumulation (N);
- Fr = Froude number (-);
- Frd = Froude number downstream the obstruction location (-);
- Fr_L = Froude number of logs (-);
- Fru = Froude number upstream the obstruction location (-);
- F_x = x- (streamwise) component of the total force exerted on the pier-debris (N);
- g = gravitational acceleration (m/s^2);
- h = flow depth downstream of the pier (m);

- H = debris accumulation height (m);
- H/h = depth ratio (-);
- $h_{c\text{-}d}$ = vertical distance from the free surface to the centroid of the area A_d (m);
- $h_{c\text{-}u}$ = vertical distance from the free surface to the centroid of the area A_u (m);
- h_{cA} = vertical distance from the free surface to the centroid of the area at cross-section A (m);
- h_{cB} = vertical distance from the free surface to the centroid of the area at cross-section B (m);
- K = debris accumulation length in the streamwise direction (m);
- k = Yarnell's pier shape coefficients (-);
- L = length of the longest log (-);
- F_{pA} = area-integrated hydrostatic forces on the upstream section A (N/m^2);
- F_{pB} = area-integrated hydrostatic forces on the downstream section B (N/m^2);
- Re = Reynolds number (-);
- S_b = bank slope (m/m);
- S_F = safety factor for the probability of scour depth being exceeded during a flood event (-);
- T^*_d = effective height of the debris accumulation (m);
- U = reference streamwise velocity of the flow (m/s);
- W = debris accumulation width (m);
- α = obstructed area of the pier divided by the total obstructed area (-);
- ρ = flow water density (kg/m^3);
- Φ_{angle} = alignment factor (m);
- Φ_{depth} = flow depth factor (-);
- Φ_{shape} = shape factor (-);
- $\Phi_{velocity}$ = velocity factor at piers (-); and
- ω = ratio of velocity head to depth downstream the pier (-).